3052 *Macromolecules* **2010**, *43*, 3052–3060
DOI: 10.1021/ma902191e

Macromolecules
ARTICLE

Theoretical Predictions on Normal Stresses under Shear Flow in Transient Networks of Telechelic Associating Polymers

Tsuyoshi Koga* and Fumihiko Tanaka

Department of Polymer Chemistry, Graduate School of Engineering, Kyoto University, Katsura, Kyoto 615-8510, Japan

Received October 3, 2009; Revised Manuscript Received December 12, 2009

ABSTRACT: This paper studies the behavior of the normal stresses in associated networks composed of telechelic polymers under steady shear flow on the basis of a transient network theory. We numerically show that the first and second normal stress coefficients reveal thickening as a function of shear rate, and that the sign of the second normal stress coefficient changes depending on the nonlinearity in the chain tension, the dissociation rate of the associative groups from junctions, and the shear rate. By analytic calculation, we show that, in the limit of small shear-rate, the sign inversion occurs by the competition between the nonlinear stretching and dissociation of associative groups. Thus, the molecular mechanism of the sign inversion is shown to be similar to that of thickening of the shear viscosity. We also show that thickening of the first normal stress coefficient has a similar molecular origin. The theoretical predictions on thickening of the first normal stress coefficient, and on the positivity of the second normal stress coefficient are confirmed by molecular dynamics simulations of a bead−spring model.

1. Introduction

Structure formation and dynamics of associating polymers have been of great interest, not only because of their scientific importance, but also because of their potential applications in diverse fields such as paints, coatings, cosmetics, and drug release formulations.[1−4] Typical examples are polymers with short hydrophobic chains attached at both chain ends (telechelic polymers) such as hydrophobic ethoxylated urethane (called HEUR),[5−13] hydrophobic poly(*N*-isopropylacrylamide),[14−16] etc. Telechelic associating polymers form flower-like micelles in dilute solution with a core of associative groups and many petals of loop chains. With increasing the polymer concentration, they are bridged by intermicellar association of polymers, leading to the formation of transient networks, where association and dissociation of junctions are possible by thermal motion of molecules and applied deformations.

The formation of transient networks is considered to be the origin of characteristic rheological properties of this system, which have been studied in many experimental,[5−13] theoretical,[17−24] and computational studies.[25−28] In the linear regime, the dynamic mechanical moduli shows a simple behavior described by a Maxwell model with a single relaxation time, which is attributed to the dissociation of associative groups from micellar junctions.[6,17,18] In contrast to the simple linear responses, complex rheological properties are observed in nonlinear regime, such as shear thickening,[9−12,19−27] network fracture,[11,27] and strain hardening.[10,30−32]

From a theoretical viewpoint, theories of transient networks have been developed to account for the characteristic rheological properties. The transient network theory was initially proposed by Green and Tobolsky[33] and later developed by Lodge[34] and Yamamoto.[35] One of us and Edwards[17,18] (referred to as TE) developed their theory for networks made up of telechelic associating polymers, and succeeded in explaining the molecular mechanism of Maxwellian behavior of the dynamic mechanical moduli and shear shinning behavior of the steady shear viscosity. Following this paper, to explain the shear-thickening behavior of the viscosity, the theory has been extended by including the effects of free chains,[19] incomplete relaxation of dangling chains,[20,21,23] and nonlinear stretching of elastically active chains.[20−24] A nonaffine transient network theory was also developed to eliminate the assumption of the affine deformation of network junctions assumed in the TE theory.[29]

Despite considerable research on the linear dynamic response and the stationary viscosity as above, no systematic studies on normal stresses of associating polymers has been reported so far, except for a few results, i.e., TE[18] calculated the first and second normal stress differences using Gaussian chains, and a few experimental[12] and computational[25,26] results on the first normal stress difference were reported. It is well-known that the normal stresses play an important role in peculiar rheological phenomena observed in viscoelastic liquids, such as the Weissenberg effect, the Poynting effect, etc.[36,37] It is interesting to study normal stress effects in associating polymers which possess characteristic rheological properties. We therefore study here the normal stresses of telechelic associating polymers under steady shear flow on the basis of a transient network theory including nonlinear stretching effect of bridge chains. In the recent studies, we have developed an effective and accurate theoretical method to calculate the stress tensor from the time evolution equation for the distribution function of bridge chains appeared in the theory[29] and utilized it for a quantitative comparison between theory and experiment.[32] We apply it to the normal stresses of telechelic associating polymers under steady shear flow in the present study.

2. Transient Network Theory

We consider transient networks made up of telechelic polymers carrying short hydrophobic groups at their chain ends (Figure 1). Let ν be the number of chains in a unit volume, n the number of statistical units on a middle chain, and a the size of the statistical repeat unit. The total length of the middle chain is given by $L \equiv na$.

There are fundamentally three kinds of chains in such networks: bridge chain (elastically effective chain), dangling chain, and loop chain. A bridge chain connects two different junctions,

*Corresponding author.

 Published on Web 03/01/2010

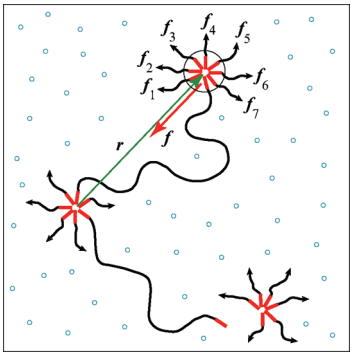

Figure 1. Bridge chain with the end-to-end vector **r**, and a dangling chain with one free end in a transient network made up of telechelic associating polymers. Tensions **f** from the chains act at the micellar junction.

while a dangling chain has one free end. There may be many loops attached to the junctions, but we neglect them in this study for simplicity because their effect is only to reduce the number of chains in the network from the total number given by the polymer concentration to the effective number governed by the thermodynamic equilibrium condition.

We consider the network subjected under a time-dependent deformation described by the tensor $\hat{\lambda}(t)$. Let $\psi(\mathbf{r},t)$ be the number of bridge chains per unit volume at time t whose end-to-end vector is given by **r**, and let $\phi(\mathbf{r},t)$ be that of the dangling chain (see Figure 1). Time evolution of the distribution function of bridge chains, $\psi(\mathbf{r},t)$, and that of dangling chains, $\phi(\mathbf{r},t)$, can be written as[29]

$$\frac{\partial \psi(\mathbf{r},t)}{\partial t} + \nabla[\bar{\mathbf{v}}\psi(\mathbf{r},t)] = -\beta(\mathbf{r})\psi(\mathbf{r},t) + \alpha(\mathbf{r})\phi(\mathbf{r},t) \quad (2.1a)$$

$$\frac{\partial \phi(\mathbf{r},t)}{\partial t} = D_1\nabla\cdot[\nabla + \mathbf{f}/k_BT]\phi(\mathbf{r},t) + \beta(\mathbf{r})\psi(\mathbf{r},t) - \alpha(\mathbf{r})\phi(\mathbf{r},t) \quad (2.1b)$$

where $\beta(\mathbf{r})$ is the chain dissociation rate of bridge chain, i.e., the probability per unit time for an end chain to dissociate from the junction, and $\alpha(\mathbf{r})$ is the recombination rate from a dangling chain to a bridge chain, i.e., the probability per unit time for a free end to catch a junction in the neighborhood at the position **r**. $\mathbf{f}(\mathbf{r})$ is the tension acting on the chain ends. The functional form of $\beta(\mathbf{r})$, $\alpha(\mathbf{r})$, and $\mathbf{f}(\mathbf{r})$ will be specified in the section of the numerical calculation (section 3). $\bar{\mathbf{v}}$ is the average velocity of junctions and D_1 is the diffusion constant of dangling ends.

In this study, we assume that the end-to-end vector of a bridge chain connecting the neighboring micellar junctions deforms affinely to the macroscopic deformation tensor $\hat{\lambda}(t)$. Thus, the average velocity $\bar{\mathbf{v}}$ of junctions is given by[17,18]

$$\bar{\mathbf{v}} = \frac{d\hat{\lambda}(t)}{dt}\cdot\hat{\lambda}(t)^{-1}\mathbf{r}(t)$$

It is possible to take the effect of nonaffine movement of junctions into account according to our previous publications,[29,32] but the theoretical treatment for the nonaffine network model is extremely complex. To get a clear physical picture for the normal stresses in this study, we use the simple affine network model as a starting point of the study of the normal stresses. The effects of nonaffine movement of junctions on the normal stresses will be addressed in our future studies.

The relaxation of dangling ends is described by the diffusion constant D_1 in eq 2.1b. In the present study, we assume, as in TE, that all the dangling chains instantaneously relax to equilibrium conformation because the relaxation time of the dangling chains is much shorter than that of the bridge chains under ordinary experimental conditions of associating polymers. Therefore, the distribution function $\phi(\mathbf{r},t)$ of dangling chains should fulfill the condition

$$(\nabla + \mathbf{f}/k_BT)\phi(\mathbf{r},t) = \mathbf{0} \quad (2.2)$$

Thus, the distribution function is given by

$$\phi(\mathbf{r},t) = \nu_d(t)\Phi(\mathbf{r}) \quad (2.3)$$

where $\nu_d(t)$ is the number of the dangling chains at time t, and

$$\Phi(\mathbf{r}) \equiv C_n \exp\left[-\int_0^{\mathbf{r}} (\mathbf{f}/k_BT)\cdot d\mathbf{r}\right] \quad (2.4)$$

with C_n being the normalization constant, is the distribution function of the end-to-end vector.

Let us first find the equilibrium solution of the coupled equations for ψ and ϕ under no deformation ($\bar{\mathbf{v}}(t) = 0$). The equilibrium distribution function of the dangling chains is given by

$$\phi_0(\mathbf{r}) = \nu_{d0}\Phi(\mathbf{r}) \quad (2.5)$$

where ν_{d0} is the number of dangling chains in a unit volume under a quiescent condition. From eq 2.1b, we find that the equilibrium distribution of the bridge chains takes the form

$$\psi_0(\mathbf{r}) = \nu_{d0}\alpha(\mathbf{r})\Phi(\mathbf{r})/\beta(\mathbf{r}) \quad (2.6)$$

Since the ratio $\beta(\mathbf{r})/\alpha(\mathbf{r})$ is the equilibrium constant $K(\mathbf{r})$ of the "chemical reaction" between bridge and dangling states, the above equation is transformed to

$$\psi_0(\mathbf{r}) = \nu_{d0}C_n \exp\left[-\int_0^{\mathbf{r}} \mathbf{F}(\mathbf{r})\cdot d\mathbf{r}\right] \quad (2.7)$$

where

$$\mathbf{F}(\mathbf{r}) \equiv \mathbf{f}/k_BT + \nabla \ln K(\mathbf{r}) \quad (2.8)$$

is the total force acting on the end of a bridge chain.

We next consider the stationary solution of the coupled equations for ψ and ϕ under a shear flow along the x-axis with a constant shear rate $\dot{\gamma}$. The average velocity is given by $\bar{\mathbf{v}}(t) = \dot{\gamma}y\mathbf{e}_x$. The equation for the distribution of the bridge chains in a steady state takes the form

$$\dot{\gamma}y\frac{\partial \psi}{\partial x} = -\beta(\mathbf{r})\psi + \nu_d\alpha(\mathbf{r})\Phi(\mathbf{r}) \quad (2.9)$$

where ν_d is the number of the dangling chains in a stationary state under the steady shear flow. To solve this equation, we introduce a function $\xi(\mathbf{r})$ by the definition $\xi(\mathbf{r}) \equiv \psi(\mathbf{r})/\psi_0(\mathbf{r})$. It gives the deviation from the equilibrium distribution in the quiescent state. Substituting into the above equation and dividing by $\psi_0(\mathbf{r})$, we find the equation for $\xi(\mathbf{r})$ as

$$\dot{\gamma}y\left(\frac{\partial}{\partial x} - \frac{x}{r}F\right)\xi = -\beta(\mathbf{r})\xi + \beta(\mathbf{r})\zeta \quad (2.10)$$

where

$$\zeta \equiv \nu_d/\nu_{d0} \quad (2.11)$$

is the number ν_d of the dangling chains in a stationary state under steady shear flow counted relative to its equilibrium value ν_{d0} without shear.

Our starting equation is then written in a compact form as

$$[\dot{\gamma}\hat{P}+\beta]\xi = \beta\zeta \tag{2.12}$$

where the operator $\hat{P}$ is defined by

$$\hat{P} \equiv y\left[\frac{\partial}{\partial x}-\frac{x}{r}F(r)\right] \tag{2.13}$$

If $\xi(\mathbf{r})$ is obtained, the ij component of the stress tensor can be calculated by

$$\sigma_{ij}(\dot{\gamma}) = \int \mathrm{d}\mathbf{r}\,(x_i f_j)(\psi_0\xi) \tag{2.14}$$

The stationary shear viscosity is obtained from the shear stress σ_{xy}

$$\eta(\dot{\gamma}) = \sigma_{xy}(\dot{\gamma})/\dot{\gamma} \tag{2.15}$$

The normal stress differences are also obtained from the normal stresses as

$$N_1 = \sigma_{xx}-\sigma_{yy} \tag{2.16a}$$

$$N_2 = \sigma_{yy}-\sigma_{zz} \tag{2.16b}$$

In the following discussion, we use the normal stress coefficient Ψ_i defined by

$$\Psi_i = \frac{N_i}{\dot{\gamma}^2} \tag{2.17}$$

3. Numerical Results of Shear and Normal Stresses

In order to overview the behavior of the normal stresses, we present the typical results obtained by the numerical calculation of eq 2.12. We first specify the functional form of $\beta(\mathbf{r})$, $\alpha(\mathbf{r})$, and $\mathbf{f}(\mathbf{r})$ for numerical calculations. The chain dissociation rate $\beta(\mathbf{r})$ is assumed to be[22,24]

$$\beta(\mathbf{r}) = \beta_0(T)[1+g\tilde{f}(\tilde{r})^2] \tag{3.1}$$

where $\beta_0(T)$ is the thermal dissociation rate, g the coupling constant between the dissociation rate and the chain tension, and $\tilde{r} \equiv r/L$. In the work by Green and Tobolsky[33], the dissociation rate was assumed to be independent of the end-to-end vector, and hence of the chain tension. We therefore go back to their theory by fixing $g = 0$ (referred to as the GT limit). The dimensionless tension $\tilde{f} \equiv fa/k_BT$ is assumed to be

$$\tilde{f}(\tilde{r}) = 3\tilde{r}\left(1+\frac{2}{3}A\frac{\tilde{r}^2}{1-\tilde{r}^2}\right) \tag{3.2}$$

The force profile is shown in Figure 2. The parameter A shows the effect of nonlinear stretching. If $A = 0$, the chain reduces to Gaussian. If $A = 1$, this profile agrees with that of a Langevin chain within a very high accuracy. The nonlinearity increases with the parameter A. Hence, we can study the effect of nonlinear elongation of the bridge chains on rheological properties of the networks by changing A. The recombination rate $\alpha(\mathbf{r})$ is assumed to be constant, and fixed at $\alpha/\beta_0 = 1$. In general, $\alpha(\mathbf{r})$ can depend on the end vector $\mathbf{r}$.[21,23,26] It was shown by the molecular dynamics simulation[27] that the recombination rate is slightly enhanced by shearing, but the effect is not significant. Furthermore, since the observed rheological properties including shear thickening can be reproduced by using a constant recombination rate α as shown in the previous publications,[22,24,32] we here use this assumption as a simplest model.

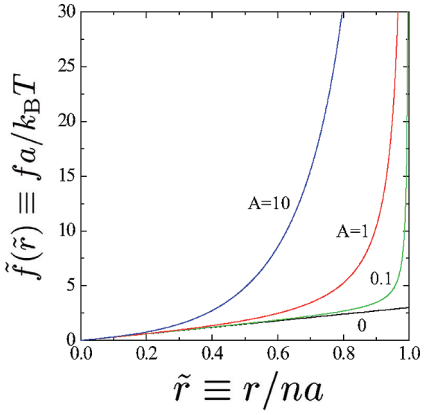

Figure 2. Tension−elongation profile of the model chain used in the transient network theory. It is Gaussian for small elongation but reveals a nonlinear stretching effect characterized by the nonlinear parameter A. For $A = 1$, the chain reduces to the Langevin chain with high accuracy.

Typical results obtained by the numerical calculation of eq 2.12 are presented in Figure.3. In what follows, the numerical values of the stresses and the shear rate are presented in units of νk_BT and β_0, respectively. The shear viscosity shows shear thinning in Figure 3a and thickening in Figure 3b. In the previous studies,[22,24] it was shown that there is a borderline on the $A-g$ plane which separates the thickening region from the thinning one (thickening diagram). Roughly, chain must be highly nonlinear (large A) and the coupling constant must be sufficiently small (small g) for thickening.

In the case of thinning Figure.3a for the shear viscosity, the first normal stress coefficient Ψ_1 also shows thinning. The sign of the second normal stress coefficient Ψ_2 remains always negative, and its absolute value decreases with increasing shear rate.

In the case of thickening Figure.3b for the viscosity, the first normal stress coefficient Ψ_1 also shows thickening as the viscosity. The second normal stress coefficient Ψ_2 has a positive sign in the small shear-rate region, and shows thickening at $\dot{\gamma} \simeq 1$. For higher shear rates, Ψ_2 rapidly decreases and changes its sign at around the shear rate where the viscosity becomes maximum. The peak appears first in Ψ_2, then Ψ_1 follows, and finally η. The reason for this order will be discussed in section 6.3 in detail.

In case of the viscosity, it was shown that thickening is caused by the nonlinear stretching of bridge chains[22,24]. In the next section, we will theoretically study the molecular origin of thickening and the sign inversion of the normal stress coefficients.

4. Analytical Solutions by Series Expansion

To study the shear-rate dependence of the stresses at small $\dot{\gamma}$ analytically, we first expand ξ and ζ in a power series of $\dot{\gamma}$.

$$\xi = \xi^{(0)}+\xi^{(1)}\dot{\gamma}+\xi^{(2)}\dot{\gamma}^2+\cdots \tag{4.1a}$$

$$\zeta = \zeta^{(0)}+\zeta^{(1)}\dot{\gamma}+\zeta^{(2)}\dot{\gamma}^2+\cdots \tag{4.1b}$$

Substituting eq 4.1 into eq 2.12, we find that the following relations hold for each order of $\dot{\gamma}$:

$$\beta\xi^{(0)} = \beta\zeta^{(0)} \tag{4.2a}$$

$$\hat{P}\xi^{(0)}+\beta\xi^{(1)} = \beta\zeta^{(1)} \tag{4.2b}$$

$$\hat{P}\xi^{(1)}+\beta\xi^{(2)} = \beta\zeta^{(2)} \tag{4.2c}$$

$$\hat{P}\xi^{(2)}+\beta\xi^{(3)} = \beta\zeta^{(3)} \tag{4.2d}$$

$$\hat{P}\xi^{(3)}+\beta\xi^{(4)} = \beta\zeta^{(4)} \tag{4.2e}$$

$$\vdots$$

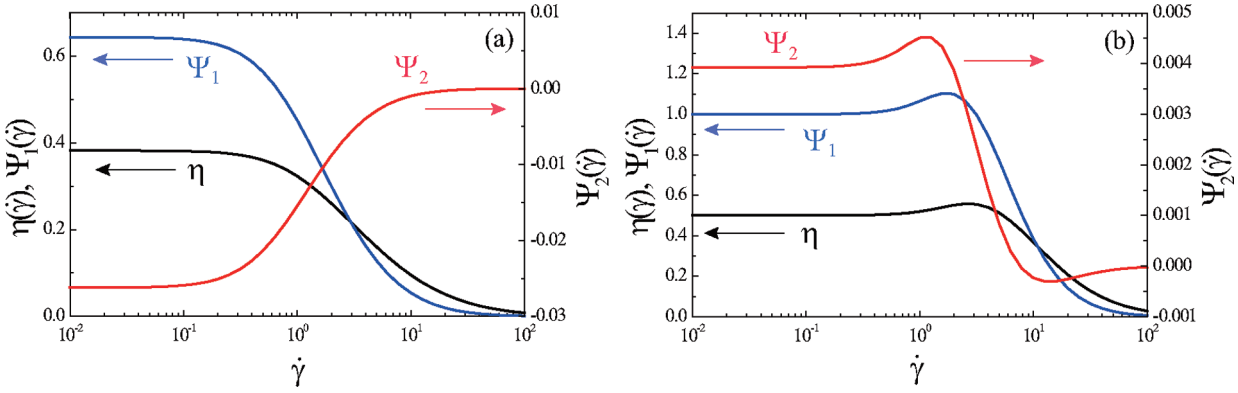

Figure 3. Stationary shear viscosity and the normal stress coefficients for the polymer chain of $n = 100$ as a function of shear rate (a) in the shear-thinning regime ($A = 1, g = 1$), and (b) in the shear-thickening regime ($A = 1, g = 0.01$).

By solving eq 4.2 order by order, we obtain

$$\xi^{(0)} = \zeta^{(0)} = 1 \tag{4.3a}$$

$$\xi^{(1)} = \Theta\frac{rF}{\beta} \tag{4.3b}$$

$$\xi^{(2)} = -\frac{1}{\beta}[\Phi^2 + \Theta^2(\hat{p} - 2)]\frac{rF}{\beta} + \zeta^{(2)} \tag{4.3c}$$

$$\xi^{(3)} = -\frac{1}{\nu}\Theta\frac{r\beta'}{\beta^2}[\Phi^2 + \Theta^2(\hat{p} - 2)]\frac{rF}{\beta} - \Theta\frac{1}{\beta}[3\Phi^2 + \Theta^2(\hat{p} - 4)](\hat{p} - 2)\frac{rF}{\beta} - \Theta rF\zeta^{(2)} \tag{4.3d}$$

where

$$\zeta^{(2)} = \frac{1}{\nu}c_{20}\int \mathrm{d}r\, \psi_0\frac{r^4F\beta'}{\beta^3} \tag{4.4}$$

and β' and β'' stand for $\mathrm{d}\beta/\mathrm{d}r$ and $\mathrm{d}^2\beta/\mathrm{d}r^2$, respectively. The odd-order terms of ζ, i.e., $\zeta^{(1)}$ and $\zeta^{(3)}$, vanish due to the symmetry. The fourth-order term $\xi^{(4)}$ is given in Appendix A. In these equations, angular factors $\Theta(\theta,\phi)$ and $\Phi(\theta,\phi)$ are separated as the prefactors of the radial differential operator $\hat{p}$ on moving to spherical coordinates. Definitions of the radial opeator $\hat{p}$ and the angular factors Θ, Φ are described in detail in Appendix A. The numerical coefficient c_{20} arising from the angular integral is also defined in Appendix A.

Upon substituting these results into eq 2.14, we obtain the series expansion of the stress tensor with respect to shear rate

$$\sigma_{ij} = \sigma_{ij}^{(0)} + \sigma_{ij}^{(1)}\dot\gamma + \sigma_{ij}^{(2)}\dot\gamma^2 + \cdots \tag{4.5}$$

5. Shear Stress

We first present the results on the shear viscosity. Although this problem has been already studied in the previous publications,[22,24] the analytical expression for the shear viscosity obtained by our new method is written in a well-organized form compared to the previous one, which facilitates understanding of the molecular origin of shear thickening. The consideration on the shear viscosity is also useful for the normal stresses in the following sections.

We calculate the series expansion of the shear stress σ_{xy} up to the third order term $\sigma_{xy}^{(3)}$. Since the even-order terms are zero due to the symmetry, the shear viscosity is written as

$$\eta(\dot\gamma) = \sigma_{xy}^{(1)} + \sigma_{xy}^{(3)}\dot\gamma^2 + \cdots \tag{5.1}$$

where the coefficients are explicitly given as

$$\sigma_{xy}^{(1)} = c_{20}\int \mathrm{d}r\, \psi_0\frac{r^4fF}{\beta} \tag{5.2a}$$

$$\sigma_{xy}^{(3)} = c_{40}\int \mathrm{d}r\, \psi_0\frac{r^6fF}{\beta^3}\left(\frac{f'}{f} - \frac{1}{r}\right)\left(F - \frac{F'}{F} + \frac{1}{r}\right) + c_{40}\int \mathrm{d}r\, \psi_0\frac{r^6fF}{\beta^3}\frac{\beta'}{\beta}\left(\frac{f'}{f} - \frac{1}{r}\right) - c_{40}\int \mathrm{d}r\, \psi_0\frac{r^6fF}{\beta^3}\frac{\beta'}{\beta}\left(F - \frac{F'}{F} + \frac{4}{r} + \frac{\beta'}{\beta}\right) + \zeta^{(2)}\sigma_{xy}^{(1)} \tag{5.2b}$$

where f' stands for $\mathrm{d}f/\mathrm{d}r$. The first term $\sigma_{xy}^{(1)}$ corresponds to the zero-shear viscosity η_0, which is always positive. The numerical coefficient c_{40} is defined in Appendix A.

The shear-rate dependence of the shear viscosity is determined by the sign of $\sigma_{xy}^{(3)}$. If $\sigma_{xy}^{(3)}$ is positive, η increases with shear rate, which indicates shear thickening. Therefore, we can judge by the sign of $\sigma_{xy}^{(3)}$ whether the viscosity shows thickening or not.[22,24] In order to show how the condition for shear thickening depends on the parameters g and A, we draw the thickening and thinning regions on the $A-g$ plane in Figure 4 on the basis of the sign of $\sigma_{xy}^{(3)}$.

To understand the molecular mechanism of shear thickening, we focus on the two factors, $(f'/f - 1/r)$ and β', in eq 5.2b. Using the force profile eq 3.2, the first one can be written as

$$\frac{f'}{f} - \frac{1}{r} = \frac{4A\tilde{r}}{3na(1 - \tilde{r}^2 + 2A\tilde{r}^2/3)(1 - \tilde{r}^2)} \tag{5.3}$$

This is 0 for Gaussian chains ($A = 0$) and positive for nonlinear chains ($A > 0$). On the other hand,

$$\beta' = 2\beta_0 gff' \tag{5.4}$$

is 0 in the GT limit ($g = 0$).

By using these properties, we consider some simple cases. In the GT limit ($g = 0$) of Gaussian chains ($A = 0$), $\sigma_{xy}^{(3)} = 0$. This corresponds to the boundary between the thickening and thinning regions on the $A-g$ plane (Figure.4b). If g increases for Gaussian chains ($A = 0$), $\sigma_{xy}^{(3)}$ becomes negative, which shows thinning. On the other hand, if A increases in the GT limit ($g = 0$), $\sigma_{xy}^{(3)}$ becomes positive showing thickening. This indicates that shear thickening is caused by the nonlinear stretching of bridge chains.

In general, the sign of $\sigma_{xy}^{(3)}$ is considered to be determined by competition between the nonlinear stretching and the breakage of bridge chains. The former is characterized by the parameter A

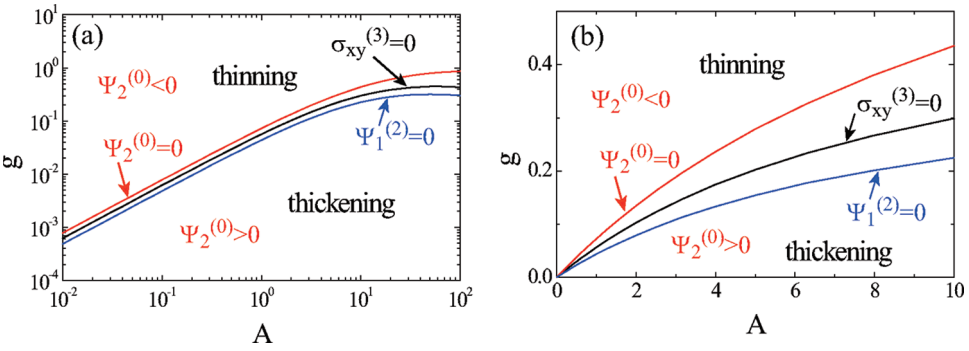

Figure 4. State diagram of thickening of the shear viscosity and the first normal stress coefficient, and of the sign inversion of the second normal stress coefficient for the polymer chain of $n = 100$ (a) in double logarithmic scale and (b) in linear scale.

and the latter by g. If bridge chains are stretched by the shear deformation, a large tension is created because of its nonlinearity expressed by A. This contributes to the increase in the shear stress. Simultaneously, the chain breakage rate becomes large due to the coupling with the tension, leading to the decrease in the number of bridge chains, and thus the shear stress. If the effect of the chain stretching is superior to that of the chain breakage, shear thickening occurs.

6. Normal Stresses

We next consider the normal stress differences. By using the series expansion of ξ eq 4.1a, we find

$$N_i = N_i^{(2)}\dot{\gamma}^2 + N_i^{(4)}\dot{\gamma}^4 + N_i^{(6)}\dot{\gamma}^6 + \cdots \tag{6.1a}$$

$$\Psi_i = \Psi_i^{(0)} + \Psi_i^{(2)}\dot{\gamma}^2 + \Psi_i^{(4)}\dot{\gamma}^4 + \cdots \tag{6.1b}$$

where $\Psi_i^{(j)} = N_i^{(j+2)}$. The odd-order terms are zero due to the symmetry.

6.1. Sign of Normal Stresses in the Small Shear-Rate Limit. Here we consider the first term $\Psi_i^{(0)}$ in the series expansion of the normal stress coefficients. By using $\xi^{(2)}$, we find

$$\Psi_i^{(0)} = -c_{02}^{(i)}\int \mathrm{d}r\,\psi_0\frac{r^4fF}{\beta^2} - c_{20}^{(i)}\int \mathrm{d}r\,\psi_0\frac{r^5fF}{\beta^2}\left(\frac{F'}{F} - F - \frac{1}{r} - \frac{\beta'}{\beta}\right) \tag{6.2}$$

In the case of the first normal stress coefficient ($c_{02}^{(1)} = -8\pi/15$, $c_{20}^{(1)} = 0$), we have

$$\Psi_1^{(0)} = \frac{8\pi}{15}\int \mathrm{d}r\,\psi_0\frac{r^4fF}{\beta^2} \tag{6.3}$$

This shows that $\Psi_1^{(0)}$ is always positive.

In the case of the second normal stress coefficient ($c_{20}^{(2)} = 8\pi/105$, $c_{02}^{(2)} = 8\pi/15 = 7c_{20}^{(2)}$), we have

$$\Psi_2^{(0)} = c_{20}^{(2)}\int \mathrm{d}r\,\psi_0\frac{r^5fF}{\beta^2}\left(\frac{f'}{f} - \frac{1}{r}\right) - c_{20}^{(2)}\int \mathrm{d}r\,\psi_0\frac{r^5fF}{\beta^2}\frac{\beta'}{\beta} \tag{6.4}$$

The first term is always zero for Gaussian chain ($A = 0$), while the second term is zero in the GT limit ($g = 0$). Therefore, $\Psi_2^{(0)} = 0$ in the GT limit of Gaussian chains. If $g > 0$ and $A = 0$, $\Psi_2^{(0)} < 0$ by the contribution from the second term. These results for Gaussian chains are consistent with those obtained by TE[18]. On the other hand, in the GT limit ($g = 0$) of nonlinear chains ($A > 0$), $\Psi_2^{(0)}$ becomes positive by the contribution from the first term.

In general, the sign of the second normal stress coefficient is determined by competition between the first and second terms. If the contribution from the nonlinear stretching is superior to that of the chain breakage, $\Psi_2^{(0)}$ becomes positive. This molecular mechanism is similar to that of shear thickening of the viscosity. Indeed, there is a strong correlation between these two phenomena as shown in Figure 4; the line for $\Psi_2^{(0)}$ lies close to the line for $\sigma_{xy}^{(3)}$.

6.2. Thickening of Normal Stress Coefficients. To discuss the shear-rate dependence of the normal stress coefficients, we next consider the second term $\Psi_i^{(2)}$ in the series expansion eq 6.1b. After straightforward but tedious calculation, we find that $\Psi_i^{(2)}$ is given as

$$\Psi_i^{(2)} = \Psi_i^{(2.1)} + \Psi_i^{(2.2)} \tag{6.5a}$$

$$\Psi_i^{(2.1)} = \int \mathrm{d}r\,\psi_0\frac{r^6fF}{\beta^4}\left\{\left(48c_{22}^{(i)} - 80c_{40}^{(i)} - 3c_{04}^{(i)}\right)\frac{1}{r} + \left(6c_{22}^{(i)} - 19c_{40}^{(i)}\right)\frac{f'}{f} - c_{40}^{(i)}\frac{rf''}{f}\right\}\left(\frac{F'}{F} - F - \frac{1}{r} - \frac{\beta'}{\beta}\right) \tag{6.5b}$$

$$\Psi_i^{(2.2)} = \int \mathrm{d}r\,\psi_0\frac{r^7fF\beta'}{\beta^5}\left\{\left[\left(-8c_{22}^{(i)} + 29c_{40}^{(i)}\right)\frac{1}{r} + c_{40}^{(i)}\left(3\frac{f'}{f} - 3\frac{\beta'}{\beta} + \frac{\beta''}{\beta'}\right)\right]\left(\frac{F'}{F} - F - \frac{1}{r} - \frac{\beta'}{\beta}\right) + \frac{1}{r}\left[\left(-c_{22}^{(i)} + c_{04}^{(i)}\right)\frac{1}{r} + c_{22}^{(i)}\left(-3\frac{\beta'}{\beta} + \frac{\beta''}{\beta'}\right)\right]\right\} + \zeta^{(2)}\Psi_i^{(0)} \tag{6.5c}$$

where f'' stands for $\mathrm{d}^2f/\mathrm{d}r^2$.

In the case of the first normal stress difference ($c_{22}^{(1)} = -8\pi/315$, $c_{40}^{(1)} = 0$, $c_{04}^{(1)} = -16\pi/35$), eqs 6.5b and 6.5c are written as

$$\Psi_1^{(2.1)} = \frac{16\pi}{105}\int \mathrm{d}r\,\psi_0\frac{r^6fF}{\beta^4}\left(\frac{f'}{f} - \frac{1}{r}\right)\left(F + \frac{1}{r} - \frac{F'}{F} + \frac{\beta'}{\beta}\right) \tag{6.6a}$$

$$\Psi_1^{(2.2)} = -\frac{8\pi}{315}\int \mathrm{d}r\,\psi_0\frac{r^6fF\beta'}{\beta^5}\left(8F - 8\frac{F'}{F} + \frac{25}{r} + 5\frac{\beta'}{\beta} + \frac{\beta''}{\beta'}\right) + \zeta^{(2)}\Psi_1^{(0)} \tag{6.6b}$$

We here consider some simple cases using the GT limit and Gaussian chains. We find $\Psi_1^{(2.1)} = 0$ for Gaussian chains

($A = 0$) and $\Psi_1^{(2.2)} = 0$ in the GT limit ($g = 0$). Therefore, $\Psi_1^{(2)} = 0$ in the GT limit of Gaussian chains.

If $g > 0$ and $A = 0$, the first term in $\Psi_1^{(2.2)}$ is negative while the second term $\zeta^{(2)}\Psi_1^{(0)}$ is always positive. By the numerical calculation, it is shown that $\zeta^{(2)}\Psi_1^{(0)}$ is smaller than the first term. Therefore, $\Psi_1^{(2)} < 0$, indicating that the first normal stress coefficient shows shear thinning for Gaussian chains.

In the GT limit ($g = 0$) of nonlinear chain ($A > 0$), $\Psi_1^{(2.1)} > 0$ and hence $\Psi_1^{(2)} > 0$. This indicates that thickening of the first normal stress coefficient occurs due to the effect of nonlinear stretching of bridge chains. The mechanism of thickening of the first normal stress coefficient is similar to that of the viscosity and the sign inversion of the second normal stress coefficient. Figure 4 clearly shows that the borderline for thickening of Ψ_1 has a similar tendency to those for thickening of the viscosity and the sign inversion of Ψ_2.

We next consider the second normal stress coefficient. By using the values for the second normal stress coefficient, $c_{22}^{(2)} = 16\pi/315$, $c_{40}^{(2)} = 16\pi/1155$, $c_{04}^{(2)} = 16\pi/35$, we find

$$\Psi_2^{(2.1)} = -\frac{16\pi}{385}\int \mathrm{d}r\, \psi_0 \frac{r^6 f F}{\beta^4}\left(\frac{f'}{f} - \frac{1}{r} - \frac{1}{3}\frac{rf''}{f}\right)\left(F + \frac{1}{r} - \frac{F'}{F} + \frac{\beta'}{\beta}\right) \tag{6.7a}$$

$$\Psi_2^{(2.2)} = \frac{16\pi}{3465}\int \mathrm{d}r\, \psi_0 \frac{r^7 f F \beta'}{\beta^5}\left\{\left[\frac{1}{r} - 9\left(\frac{f'}{f} - \frac{\beta'}{\beta} + \frac{1}{3}\frac{\beta''}{\beta'}\right)\right]\times \left(F + \frac{1}{r} - \frac{F'}{F} + \frac{\beta'}{\beta}\right) + \frac{11}{r}\left(\frac{8}{r} - 3\frac{\beta'}{\beta} + \frac{\beta''}{\beta'}\right)\right\} + \zeta^{(2)}\Psi_2^{(0)} \tag{6.7b}$$

In Figure 5, we show the positive and negative regions of $\Psi_2^{(2)}$ on the $A-g$ plane. The behavior of $\Psi_2^{(2)}$ is quite different from the previous cases.

Here we discuss the GT limit ($g = 0$), where $\Psi_2^{(2.2)} = 0$. If the chain is Gaussian, $\Psi_2^{(2.1)} = 0$. In the case of nonlinear chain ($A > 0$), it is shown that $\Psi_2^{(2.1)} > 0$ by using eq 3.2. Since the first term $\Psi_2^{(0)}$ in the expansion is positive in the GT limit, the absolute value of Ψ_2 increases with shear rate.

In general, since the sign of the second normal stress difference in the small shear-rate limit changes depending on A and g as shown in Figures.4 and 6, it is necessary to define thickening or thinning in the second normal stress coefficient for its absolute value. If we define thickening as a case where the absolute value of Ψ_2 increases, the shear-thickening regions for Ψ_2 correspond to the region where $\Psi_2^{(0)} > 0$ and $\Psi_2^{(2)} > 0$, and that where $\Psi_2^{(0)} < 0$ and $\Psi_2^{(2)} < 0$ on the $A - g$ plane in Figure 5.

6.3. Order of Thickening and Sign Inversion. Finally, we discuss the shear rates in which the viscosity and the normal stress coefficients take maximum. To obtain the maximum shear rates analytically, higher order terms in the series expansion of the stress tensor are necessary. Since it is difficult to obtain the higher order terms, we study this problem by the numerical integration of eq 2.12.

Let $\dot{\gamma}_{\max}(\eta)$ and $\dot{\gamma}_0(\Psi_i)$ be the shear rates at which the viscosity and the ith normal stress coefficients take maximum, respectively. Also, $\dot{\gamma}_0(\Psi_2)$ is defined as the shear rate where the sign inversion occurs in the second normal stress coefficient. The numerical results are shown in Figure 7, where the shear rates are scaled by $\dot{\gamma}_{\max}(\eta)$. In Figure 7a, the ratio of the characteristic shear rates are shown as a function of A at $g = 0.001$. With increasing A, $\dot{\gamma}_{\max}(\Psi_i)/\dot{\gamma}_{\max}(\eta)$'s decrease, while $\dot{\gamma}_0(\Psi_2)$ increases. In Figure 7b, the ratio of the shear rates are shown as a function of g at $A = 1$. Except for the increase in $\dot{\gamma}_0(\Psi_2)/\dot{\gamma}_{\max}(\eta)$ at small g, the ratios are almost constant independent of g. This tendency is commonly observed in other values of A. Therefore, we conclude that the ratios of the maximum shear rates are predominantly determined by A.

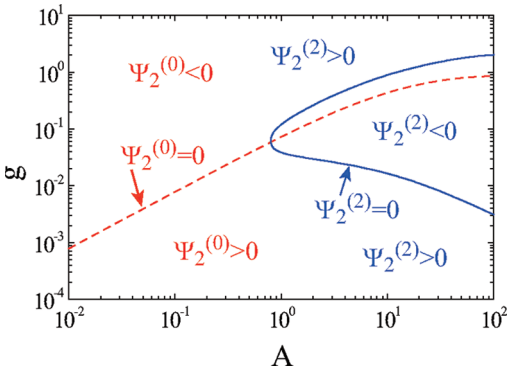

Figure 5. State diagram of the sign inversion and thickening of the second normal stress coefficient in double logarithmic scale ($n = 100$).

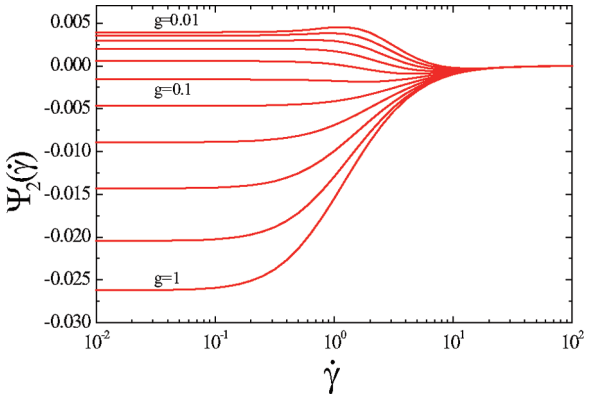

Figure 6. Second normal stress coefficient obtained by the numerical calculation as a function of shear rate. The coupling constant g is changed from curve to curve, ranging from 0.01 to 1 at $n = 100$, $A = 1$.

As for the order of the occurrence of thickening and the sign inversion, Figure 7 shows $\dot{\gamma}_{\max}(\Psi_2) < \dot{\gamma}_{\max}(\Psi_1) < \dot{\gamma}_{\max}(\eta)$ except for the small-A region ($A < 0.15$). The sign inversion occurs at a larger shear rate than that of shear thickening of the viscosity.

7. Weissenberg Effect

We here consider the Weissenberg effect[36,37] expected in telechelic associating polymers. The condition for the rod-climbing phenomenon in slow flows is given by[38]

$$N_2/N_1 > -1/4 \tag{7.1}$$

It is shown that this relation is satisfied for reasonable parameters in the present theory (Figure 8). To violate the relation eq 7.1, the coupling constant g should be larger than 5×10^4, which is much larger than those obtained by the fitting with experiments (eq 9.4b and refs 31 and 32). Therefore, the rod-climbing phenomenon can be observed in telechelic associating polymers. Since the magnitude of the rod-climbing is proportional to $(N_1 + N_2)/4$, the rod-climbing effect is enhanced by increasing the rotational speed of rods in the shear-thickening region, and then suddenly disappear at a higher speed due to strong shear shinning. Flow instabilities at larger shear rates, such as fracture of networks and shear

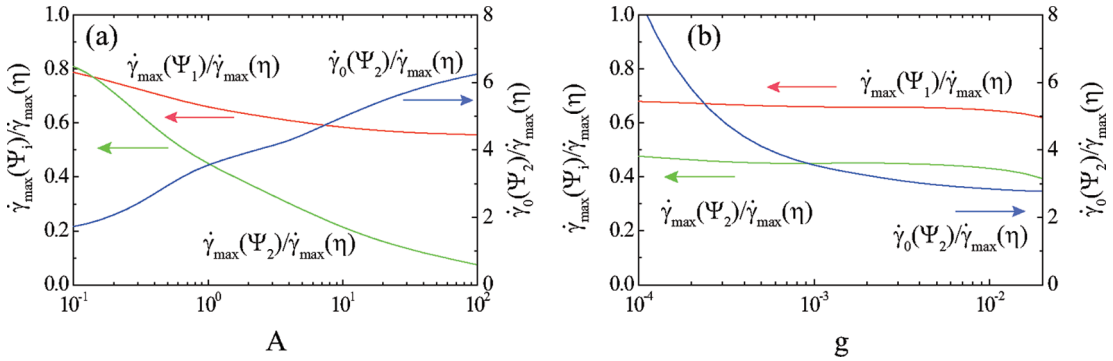

Figure 7. Characteristic shear rates of the normal stress coefficients, $\dot{\gamma}_{max}(\Psi_i)$, $\dot{\gamma}_{max}(\Psi_2)$, and $\dot{\gamma}_0(\Psi_2)$, scaled by $\dot{\gamma}_{max}(\eta)$ for the polymer chain of $n = 100$ as a function of the nonlinear parameter A (a) and of the coupling constant g (b).

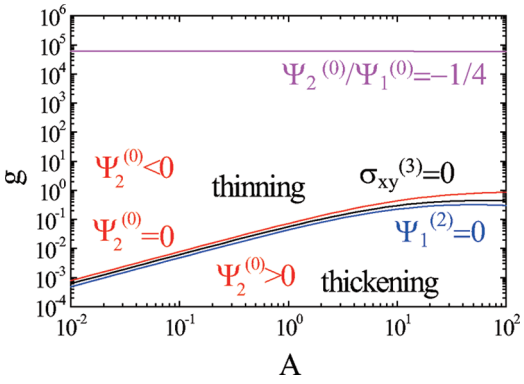

Figure 8. Condition for the rod-climbing effect on the $A-g$ plane together with those for thickening and the sign inversion of the normal stress coefficients ($n = 100$).

banding,[11,27] are expected to induce more drastic changes in macroscopic phenomena by normal stress effects.

8. Simulation Results

To confirm the theoretical predictions, we have calculated the normal stresses by using a molecular dynamics simulation of a bead−spring model.[27] Beads are connected by the finitely extensible nonlinear elastic springs. Each chain carries end beads interacting with cross-linkers through associative potential with strength ε_a. Time, length, and energy are scaled by the usual Lennard-Jones units. Details of the model and simulation method have been described in ref 27. In Figure 9, we present the normal stress coefficients in the case that shear thickening of the shear viscosity is observed ($\varepsilon_a/k_BT = 7.5$ in ref 27).

The first normal stress coefficient shows thickening at moderate shear rates at around $\dot{\gamma} \simeq 0.3$, and rapidly decreases compared to η at larger shear rates. The maximum shear rate for Ψ_1, $\dot{\gamma}_{max}(\Psi_1)$, is smaller than $\dot{\gamma}_{max}(\eta)$, which agrees with the theoretical prediction. The second normal stress coefficient Ψ_2 takes positive values as predicted by the theory. It is difficult to determine whether thickening of Ψ_2 occurs or not due to large errors. At larger shear rates, Ψ_2 decreases and is close to zero at $\dot{\gamma} = 0.1$. Although Ψ_2 is expected to be negative according to the theoretical result (Figure 3b), it is difficult to obtain the normal stresses with high accuracy at larger shear rates $\dot{\gamma} > 0.1$ due to the occurrence of fracture of networks.[27] Details of the simulation results on the normal stresses will be discussed in our forthcoming paper.

It should be noted that the numerical results showing thickening of the first normal coefficient were presented in refs 25 and 26, where thickening is caused by the increase in the number of bridge chains by shear flow. Therefore, the molecular mechanism of thickening is different from that of the present case (nonlinear stretching of bridge chains).

9. Comparison with Experiments

We compare the theoretical results with the experimental ones. Pellens et al.[12] studied the first normal stress coefficient of HEUR with hexadecyl end groups. The experimental results are shown in Figure 10. They reported that, in the small shear-rate region, the measured values of the first normal stress coefficient Ψ_1 satisfies the relation obtained by the linear viscoelasticity:

$$\Psi_1(\dot{\gamma}) = \frac{2G'(\omega)}{\omega^2} \tag{9.1}$$

The measured values deviates from the relationship eq 9.1 at higher shear rates, but does not increase with shear rate even in the region where the shear viscosity exhibits shear thickening.

This experimental result can be interpreted by the theoretical result shown in Figure 4, in which there is a region where the shear viscosity increases with shear rate whereas the first normal stress coefficient decreases. We consider that the experimental condition for the data in Figure 10 is located in this region. To compare more quantitatively, we also present the theoretical results in Figure 10. The parameters in the theory is estimated by the molecular properties, the experimental conditions, and the fitting with the experimental results on the dynamic mechanical moduli and the nonlinear steady viscosity. The number of segments of the PEO main chain is estimated as $n = 119$ on the basis of the literature value of the Kuhn length $a = 0.7$ nm[39] and the length of a monomeric unit $a_0 = 0.36$ nm. From the polymer concentration $c = 2.9$ wt % and the molecular weight $M_w = 20\,000$, the number density ν of polymers is

$$\nu = \frac{cN_A}{M_w} = 8.99 \times 10^{23}\ \mathrm{m}^{-3} \tag{9.2}$$

In the case of $T = 293$ K, we have

$$\nu k_B T = 3637\ \mathrm{Pa} \tag{9.3}$$

For the parameter A characterizing the nonlinearity in the chain tension, we fitted eq 3.2 to the data of the tension−elongation curve obtained directly by AFM measurement[39] and found $A = 5$ for the optimal value. By the fitting with the experimental results on the dynamic mechanical moduli and the nonlinear steady viscosity, we have

$$\beta_0 = 9.5\ \mathrm{s}^{-1} \tag{9.4a}$$

$$g = 0.16 \tag{9.4b}$$

$$\alpha = 1.48\ \mathrm{s}^{-1} \tag{9.4c}$$

The theoretical results by using these parameter are shown in Figure 10. At high shear rates, the theoretical values are

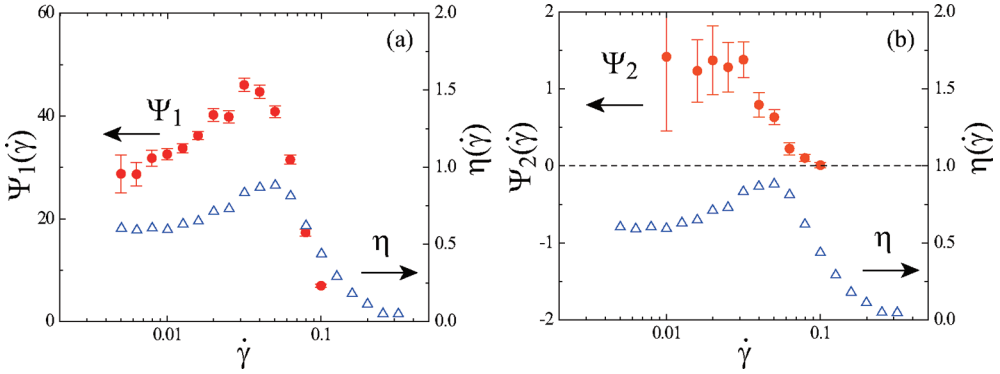

Figure 9. Normal stress coefficients obtained by molecular dynamics simulation.[27] The first and second normal stress coefficients are presented in parts a and b, respectively, together with the stationary shear viscosity as a function of the shear rate.

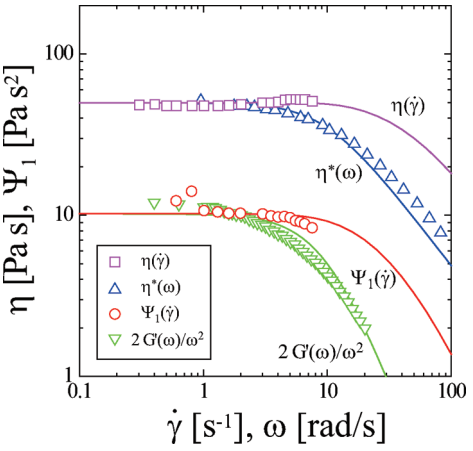

Figure 10. Comparison of the steady shear viscosity and the first normal stress coefficient between theory and experiment.[12] Experimental and theoretical results are shown by symbols and solid lines, respectively.

somewhat larger than the experiment ones, but the experimental results are well described by the theory. The obtained value $g = 0.16$ for $A = 5$ is very close to the boundary of thickening of Ψ_1. Therefore, we expect that if the experimental condition is changed to enhance the effect of the nonlinear stretching of bridge chains compared to that of the dissociation rate of associative groups, thickening of Ψ_1 should be observed. According to ref 9, shear thickening is enhanced by the increase in the length of the hydrophobic groups and the decrease in the polymer concentration. It is very interesting to measure the first normal stress coefficient of telechelic polymers with more strong hydrophobic groups at lower concentrations.

10. Conclusions and Discussion

We have studied the behavior of the normal stresses in networks composed of telechelic associating polymers under steady shear flow on the basis of the transient network theory. We numerically showed that the first and second normal stress coefficients show thickening as a function of shear rate, and that the sign of the second normal stress coefficient changes depending on the nonlinearity in the chain tension, the dissociation rate of the associative groups from junctions, and the shear rate. By analytic calculation, we showed that, in the limit of small shear-rate, the sign inversion occurs by competition between the nonlinear stretching and the dissociation of associative groups. The molecular mechanism of the sign inversion is similar to that of thickening of the viscosity. We also showed that thickening of the first normal stress coefficient has a similar molecular origin. On the other hand, thickening of the second normal stress difference is caused by other complex molecular mechanism. The theoretical predictions on thickening of the first normal stress coefficient, and on the positivity of the second normal stress coefficient are confirmed by molecular dynamics simulations of a bead−spring model.

As long as we know, there is no experimental report on thickening of the normal stress coefficients and the sign inversion of the second normal stress coefficient in telechelic associating polymers. As shown in Figure 4, the second normal stress coefficient is always positive in the region where the viscosity shows thickening. Since thickening of the viscosity widely observed in telechelic associating polymers, the positive second normal stress coefficient should be obtained by precise measurements. Once the positive second normal stress coefficient is measured, the sign inversion by the increase of the shear rate shown in Figure 3 is also expected to be observed under the same experimental condition. Detailed and precise experiments on the second normal stress difference in associating polymers are very desirable.

We finally emphasize the importance of the second normal stress coefficient in the rheology of telechelic associating polymers. To understand the molecular mechanism of rheological properties of this system, there are two important factors, i.e., the nonlinearity in the chain tension and the dissociation rate of associative groups from junctions. Although the two factors appear in the expression eq 5.2b for shear thickening of the viscosity, they are coupled in a complicated way. On the other hand, the second normal stress coefficient can be expressed by the simple sum of the two effects in the small shear-rate limit as shown in eq 6.4. This means that competition between two effects can be directly observed in the second normal stress coefficient.

Acknowledgment. This work is partly supported by a Grant-in-Aid for Scientific Research on Priority Areas "Soft Matter Physics" from the Ministry of Education, Culture, Sports, Science, and Technology of Japan, and partly supported by a Grant-in-Aid for Scientific Research (B) from the Japan Society for the Promotion of Science under Grant Number 19350057. We wish to acknowledge their support.

Appendix A. Expansion of the Distribution Function in Powers of Shear Rate

To derive the series expansion of ξ and σ_{ij}, we use polar coordinates ($x = r \sin\theta \cos\phi$, $y = r \sin\theta \sin\phi$, and $z = r \cos\theta$) and define abbreviated notations

$$\Phi \equiv \sin\theta \sin\phi, \quad \Theta \equiv \sin^2\theta \sin\phi \cos\phi$$

The operator $\hat{P}$ acts only on the functions of r. Simple calculation gives

$$\hat{P}1 = -\Theta(rF)$$

which gives ξ_1. Similarly we have

$$\hat{P}\xi_1 = [\Phi^2 + \Theta^2(\hat{p} - 2)]\frac{rF}{\beta}$$

where the operator $\hat{p}$ is defined by

$$\hat{p} \equiv r\left(\frac{\mathrm{d}}{\mathrm{d}r} - F(r)\right)$$

We then have ξ_2 in eq 4.3c. Repeating the similar operations, we find, after lengthly calculation, the higher order terms $\xi^{(3)}$ in eq 4.3 in the text and $\xi^{(4)}$:

$$\begin{aligned}\xi^{(4)} = &-\frac{1}{\beta} - \Theta^2\frac{r}{\beta^3}\left(\beta' + r\beta'' - \frac{3r\beta'^2}{\beta}\right)[\Phi^2 + \Theta^2(\hat{p} - 2)]\frac{rF}{\beta} \\ &- \Theta^2\frac{r\beta'}{\beta^3}[3\Phi^2 + \Theta^2(\hat{p} - 4)](\hat{p} - 2)\frac{rF}{\beta} \\ &- (\Phi^2 - 2\Theta^2)\frac{r\beta'}{\beta^3}[\Phi^2 + \Theta^2(\hat{p} - 2)]\frac{rF}{\beta} \\ &- 2\Theta^2\frac{r\beta'}{\beta^3}[3\Phi^2 + \Theta^2(\hat{p} - 4)](\hat{p} - 2)\frac{rF}{\beta} \\ &+ \frac{1}{\beta^2}[3\Phi^4 + 6\Theta^2\Phi^2(\hat{p} - 4) + \Theta^4(\hat{p} - 6)(\hat{p} - 4)](\hat{p} - 2)\frac{rF}{\beta} \\ &+ \zeta^{(2)}[\Phi^2 + \Theta^2(\hat{p} - 2)]\frac{rF}{\beta} + \zeta^{(4)} \qquad \text{(A.1)}\end{aligned}$$

Upon such decomposition, we are led to the following angular integrals:

$$c_{lm} \equiv \int \sin\theta\, \mathrm{d}\theta\, \mathrm{d}\phi\, \Theta^l\Phi^m$$

$$c^{(1)}_{mn} \equiv \int \sin\theta\, \mathrm{d}\theta\, \mathrm{d}\phi\, \Theta_1\Theta^m\Phi^n$$

$$c^{(2)}_{mn} \equiv \int \sin\theta\, \mathrm{d}\theta\, \mathrm{d}\phi\, \Theta_2\Theta^m\Phi^n$$

where $\Theta_1 \equiv \sin^2\theta\,(1 - 2\sin^2\phi)$ and $\Theta_2 \equiv \sin^2\theta\,(1 + \sin^2\phi) - 1$. The numerical constants arising from the angular integrals are

$$c_{20} = \frac{4\pi}{15}, \quad c_{40} = \frac{4\pi}{105}$$

$$c^{(1)}_{20} = 0, \quad c^{(1)}_{02} = -\frac{8\pi}{15}, \quad c^{(2)}_{20} = \frac{8\pi}{105}, \quad c^{(2)}_{02} = \frac{8\pi}{15}$$

$$c^{(1)}_{40} = 0, \quad c^{(1)}_{22} = -\frac{8\pi}{315}, \quad c^{(1)}_{04} = -\frac{16\pi}{35}$$

$$c^{(2)}_{40} = \frac{16\pi}{1155}, \quad c^{(2)}_{22} = \frac{16\pi}{315}, \quad c^{(2)}_{04} = \frac{16\pi}{35}$$

References and Notes

(1) *Hydrophilic Polymers: Performance with Environmental Acceptability*; Glass, J. E., Ed.; American Chemical Society: Washington, DC, 1996; Vol. *248*.
(2) *Associative Polymers in Aqueous Solution*; Glass, J. E., Ed.; American Chemical Society: Washington, DC, 2000; Vol. *765*.
(3) *Amphiphilic Block Copolymers: Self-Assembly and Applications*; Alexandridis, P., Lindman, B., Ed.; Elsevier: New York, 2000.
(4) Winnik, M. A.; Yekta, A. *Curr. Opin. Colloid Interface Sci.* **1997**, *2*, 424.
(5) Jenkins, R. D.; Silebi, C. A.; El-Asser, M. S. *Polymers as Rheology Modifiers*; ACS Symposium Series 462; American Chemical Society: Washington DC, 1991; p 222.
(6) Annable, T.; Buscall, R.; Ettelaie, R.; Whittlestone, D. *J. Rheol.* **1993**, *37*, 695.
(7) Annable, T.; Buscall, R.; Ettelaie, R.; Shepherd, P.; Whittlestone, D. *Langmuir* **1994**, *10*, 1060.
(8) Yekta, A.; Xu, B.; Duhamel, J.; Adiwidjaja, H.; Winnik, M. A. *Macromolecules* **1995**, *28*, 956.
(9) Ma, S. X.; Cooper, S. L. *Macromolecules* **2001**, *34*, 3294.
(10) Berret, J.-F.; et al. *J. Rheol.* **2001**, *45*, 477.
(11) Berret, J.-F.; Séréro, Y. *Phys. Rev. Lett.* **2001**, *87*, 048303.
(12) Pellens, L.; Corrales, R. G.; Mewis, J. *J. Rheol.* **2004**, *48*, 379.
(13) Pellens, L.; Ahn, K. H.; Lee, S. J.; Mewis, J. *J. Non-Newtonian Fluid Mech.* **2004**, *121*, 87.
(14) Kujawa, P.; Watanabe, H.; Tanaka, F.; Winnik, F. M. *Eur. Phys. J. E* **2005**, *17*, 129.
(15) Kujawa, P.; Segui, F.; Shaban, S.; Diab, C.; Okada, Y.; Tanaka, F.; Winnik, F. M. *Macromolecules* **2006**, *39*, 341.
(16) Koga, T.; Tanaka, F.; Motokawa, R.; Koizumi, S.; Winnik, F. M. *Macromolecules* **2008**, *41*, 9413.
(17) Tanaka, F.; Edwards, S. F. *Macromolecules* **1992**, *25*, 1516.
(18) Tanaka, F.; Edwards, S. F. *J. Non-Newtonian Fluid Mech.* **1992**, *43*, 247, 272, 289
(19) Wang, S. Q. *Macromolecules* **1992**, *25*, 7003.
(20) Marrucci, G.; Bhargava, S.; Cooper, S. L. *Macromolecules* **1993**, *26*, 6483.
(21) Vaccaro, A.; Marrucci, G. *J. Non-Newtonian Fluid Mech.* **2000**, *92*, 261.
(22) Indei, T.; Koga, T.; Tanaka, F. *Macromol. Rapid Commun.* **2005**, *26*, 701.
(23) Tripathi, A.; Tam, K. C.; McKinley, G. H. *Macromolecules* **2006**, *39*, 1981.
(24) Indei, T. *J. Non-Newtonian Fluid Mech.* **2007**, *141*, 18.
(25) van den Brule, B. H. A. A.; Hoogerbrugge, P. J. *J. Non-Newtonian Fluid Mech.* **1995**, *60*, 303.
(26) Hernández Cifre, J. G.; Barenbrug, Th. M. A. O. M.; Schieber, J. D.; van den Brule, B. H. A. A. *J. Non-Newtonian Fluid Mech.* **2003**, *113*, 73.
(27) Koga, T.; Tanaka, F. *Eur. Phys. J. E* **2005**, *17*, 115.
(28) Hernández Cifre, J. G.; Pamies, R.; Kjøniksen, A.-L.; Knudsen, K. D.; Nyström, B.; Garcia de la Torre, J. *J. Non-Newtonian Fluid Mech.* **2007**, *146*, 3.
(29) Tanaka, F.; Koga, T. *Macromolecules* **2006**, *39*, 5913.
(30) Kaneda, I.; Koga, T.; Tanaka, F.; Winnik, F. M. *Colloid Polym. Sci.* **2009**, *136*, 31.
(31) Koga, T.; Tanaka, F.; Kaneda, I.; Winnik, F. M. *Colloid Polym. Sci.* **2009**, *136*, 39.
(32) Koga, T.; Tanaka, F.; Kaneda, I.; Winnik, F. M. *Langmuir* **2009**, *25*, 8626.
(33) Green, M. S.; Tobolsky, A. V. *J. Chem. Phys.* **1946**, *14*, 80.
(34) Lodge, A. S. *Trans. Faraday Soc.* **1956**, *52*, 120.
(35) Yamamoto, M. *J. Phys. Soc. Jpn.* **1956**, *11*, 413. Yamamoto, M. *J. Phys. Soc. Jpn.* **1957**, *12*, 1148. Yamamoto, M. *J. Phys. Soc. Jpn.* **1958**, *13*, 1200.
(36) Lodge, A. S. *Elastic Liquids*; Academic Press: London, 1964.
(37) Bird, R. B.; Curtiss, C. F.; Armstrong, R. C.; Hassager, O. *Dynamics of Polymeric Liquids*; John Wiley & Sons: New York, 1987; Vol. *1*.
(38) Beavers, G. S.; Joseph, D. D. *J. Fluid Mech.* **1975**, *69*, 475.
(39) Oesterhelt, F.; Rief, M.; Gaub, H. E. *New J. Phys.* **1999**, *1*, 61.